electronics

MDPI

Article

Novel Synthesis Method for Microwave Parallel-Coupled Resonator Bandpass Filters

Slawomir Gruszczynski * and Krzysztof Wincza

Department of Electronics, Faculty of Computer Science, Electronics and Telecommunications, AGH University of Krakow, al. Mickiewicza 30, 30-059 Krakow, Poland; wincza@agh.edu.pl
* Correspondence: gruszczy@agh.edu.pl; Tel.: +48-12-617-56-17

Abstract

In this study, a novel synthesis method for bandpass filters is proposed. The method relies on Richard's transform and avoids approximations in circuit realizations. Thus, proper frequency responses are obtained for bandpass filters with bandwidths ranging from narrow to wide. In the presented approach, a method for removing the input and output inverters/transformers is proposed and is used to show how classic parallel-coupled resonator filters can be designed using the proposed method. Also, a degree of freedom is introduced that allows the overall impedance level of the fabricated filter to be tuned, which is used to tune the frequency response of the filter to the theoretical one. Both narrowband and wideband solutions in terms of impedance inverter realization are discussed in the paper. The theoretical investigations are confirmed by an experimental realization of two bandpass filters with parallel-coupled shorted resonators.

Keywords: bandpass filters; coupled resonator filters; edge-coupled filters; microwave filters; parallel-coupled filters

check for updates

Academic Editor: Nakkeeran Kaliyaperumal

Received: 16 July 2025
Revised: 29 July 2025
Accepted: 4 August 2025
Published: 5 August 2025

Citation: Gruszczynski, S.; Wincza, K. Novel Synthesis Method for Microwave Parallel-Coupled Resonator Bandpass Filters. *Electronics* **2025**, *14*, 3123. https://doi.org/10.3390/electronics14153123

Copyright: © 2025 by the authors. Licensee MDPI, Basel, Switzerland. This article is an open access article distributed under the terms and conditions of the Creative Commons Attribution (CC BY) license (https://creativecommons.org/licenses/by/4.0/).

1. Introduction

The design of microwave bandpass filters has a long history in the microwave community. There is a large number of recent works related to microwave filter design, and the following aspects are investigated: multi-passband filters [1,2]; filters with improved out-of-band attenuation [3,4]; quasi-elliptic filters; filters with adjustable transmission zeros [5,6]; filters with lumped and quasi-lumped elements [7,8]; filters designed using coupling matrix technique [9–11]; filters designed in monolithic technologies [12]; and advanced combline filters [13].

Early work on microwave bandpass filter design was presented by Cohn [14,15] and Matthaei [16], who showed that such filters can be designed with the use either open-ended or shorted quarter-wave-long parallel-coupled sections. Both contributors have proposed circuit transformations based on the calculation of image parameters of the corresponding filter subsections, in order to transform a prototype filter into the final design. This approach allowed for analytical calculation of the filter geometry for a given filter order and chosen approximation. However, the responses of the resulting filters closely resemble the theoretical ones for narrow bandwidths, and become distorted as the filters' relative bandwidths increase.

In [15] the author demonstrated how the response of an exemplary six-resonator filter degrades with an increasing relative bandwidth. The distortions are visible for bandwidths as narrow as 20%. Much better responses were obtained by Matthaei [16], who proposed a

competitive approach for calculating filter subcircuit parameters using image parameters. In this case, the author reported that, for a six-resonator filter, distortions appear only above relative bandwidths of around 30%. Recently, it has been reported that bandpass filters can be designed with the use of Richards' transform and wideband impedance inverters. Such an approach leads to easy realization of directly connected transmission-line filters having relatively wide bandwidths [17].

In this paper the idea presented in [17] is further developed. It is shown how a prototype circuit composed of shorted transmission lines with different characteristic impedances and ideal impedance inverters can be transformed into a circuit with shorted stubs with equal characteristic impedances. This approach allows not only for circuit simplification but also for the application of circuit identities. As a result, coupled-line sections can be introduced.

Furthermore, this paper demonstrates how the input and output sections can be rearranged using Kuroda's identities to obtain a circuit that can also be realized with coupled-line sections. Since the application of Kuroda's identities requires the substitution of a unit element in place of the ideal impedance/admittance inverter, the response of wideband filters becomes affected. However, as shown in this work, adjusting a single value of stubs' characteristic impedances solves this problem, thereby achieving an ideal frequency response.

Two practical realizations are considered in this paper. In the first, all inverters are replaced with quarter-wave-long sections. This is a narrow-band approach, suitable for filters with bandwidths up to 15%. In the second approach, broadband admittance inverters proposed in [17] are applied, enabling the design of filters with very wide bandwidths. Additionally, a condition is derived that allows the calculation of the stubs' characteristic impedance, which ensures an ideal frequency response. Therefore, filter tuning is not necessary, as long as the inverter bandwidth is sufficiently wide. This condition holds for bandwidths up to 45% when using the inverters proposed in [17]. Wider bandwidths can also be achieved, although tuning a single parameter is required to compensate for the limited bandwidth of the inverters used. An ideal frequency response can thus be obtained over an unlimited bandwidth. As a result, such filters can, for example, be utilized as pseudo-high-pass filters. The theoretical investigations are confirmed by the design of two bandpass filters: one utilizing the narrowband approach and the other employing the broadband approach.

2. General Synthesis Methods

The general synthesis method is based on the approach shown in [17], where the design of directly connected-line filters was presented. The method relies on low-pass filter prototypes that are subject to lowpass-to-highpass transformations and Richard's transformations, resulting in a bandpass microwave prototype filter (see Figure 1). Subsequently, a number of impedance inverters are introduced to convert the filter into a network in which only one type of element is present—either series open-ended subs or shunt shorted ones.

By imposing symmetry on the network in Figure 1, the number of filter-independent parameters is reduced. In particular the admittance inverter values become equal in pairs, as follows:

$$J_k = J_{n+2-k} \tag{1}$$

where n is the filter order—i.e., the number of the lumped elements in the prototype filter shown in Figure 1a—and also the number of corresponding lumped elements in the transformed filter in Figure 1b. Note that the filter in Figure 1b has undergone Richard's transformation, meaning that the lumped elements are now represented by sections of

shorted transmission lines. As shown in [17] the normalized impedances of these lines (assuming a reference impedance $Z_0 = 1\ \Omega$) can be calculated as:

$$\begin{aligned} Z_k &= \frac{1}{g_k \Omega_c} \prod_{j=1}^{k} J_j^{2(-1)^j} \text{ for } k \text{ odd} \\ Z_k &= \frac{1}{g_k \Omega_c} \prod_{j=1}^{k} J_j^{2(-1)^{j+1}} \text{ for } k \text{ even,} \end{aligned} \tag{2}$$

$k = 1$ to n. Taking Equation (1) into account, there are $(n+1)/2$ independent stub impedances and the same number of independent inverter values. Therefore, Equation (2) forms a system that can be easily solved for the J_j values, where the stub impedances Z_k can be arbitrarily assigned. In particular, all impedances can be set to the same arbitrary value Z_s giving one degree of freedom to the designer and setting the impedance of the internal sections of the filter. The J_j inverter values can be calculated as follows:

$$\begin{aligned} J_1 &= \frac{1}{\sqrt{Z_s g_1 tan(\theta)}} \\ J_2 &= \frac{J_1}{\sqrt{Z_s g_2 tan(\theta)}} \\ J_3 &= \frac{J_2}{J_1 \sqrt{Z_s g_3 tan(\theta)}} \\ J_4 &= \frac{J_3 J_1}{J_2 \sqrt{Z_s g_4 tan(\theta)}} \end{aligned} \tag{3}$$

This can be generalized as:

$$\begin{aligned} J_1 &= \frac{1}{\sqrt{Z_s g_1 tan(\theta)}} \\ J_k &= \frac{1}{\sqrt{Z_s g_k tan(\theta)}} \prod_{j=1}^{k-1} J_j^{(-1)^{j+1}} \text{ for } k \text{ even} \\ J_k &= \frac{1}{\sqrt{Z_s g_k tan(\theta)}} \prod_{j=1}^{k-1} J_j^{(-1)^{j}} \text{ for } k \text{ odd} \end{aligned} \tag{4}$$

where $k = 2 \ldots (n+1)/2$, n is the filter order (assumed to be odd due to the symmetry restriction), $\theta = \pi/2\,(1 - B/200)$. The relative bandwidth is given by $B = (f_U - f_L)/f_0$, where f_U, f_L, f_0 are upper, lower and center frequencies, respectively.

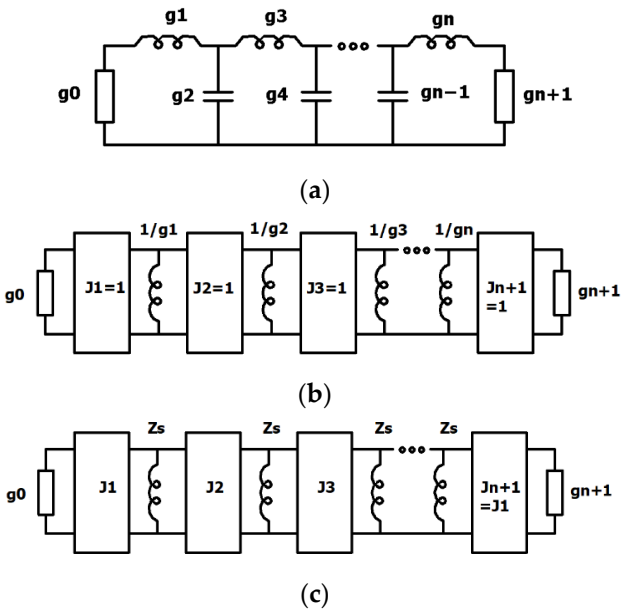

Figure 1. Schematic diagram of a lowpass prototype ladder filter (**a**); the corresponding bandpass filter, where both Richard's transform and lowpass-to-highpass transformations have been applied (**b**) [17]; the filter with recalculated inverter values and equal stub impedances *Zs* (**c**).

The presented method is general and yields a network consisting of shorted stubs and admittance inverters. The filter response is ideal, meaning that it preserves equal-ripple characteristics and the specified ripple level throughout the bandwidth B. The only restriction is that the filter order must be odd, a requirement introduced to maintain network symmetry and simplify the synthesis process—though it imposes only minimal practical limitations. Further design of the filter depends on the chosen physical realization. In this paper, parallel-coupled resonator filters are considered.

3. Parallel-Coupled Resonator Filters

3.1. General Solution

In the design of parallel-coupled resonator filters, the known circuit identity shown in Figure 2 is utilized, in which two shorted transmission-line sections connected by another section can be replaced by a parallel-coupled-line section shorted at the opposite ends. Thus, in order to convert the filter from Figure 1b into a structure that consists of parallel-coupled lines, the transmission-line stubs with impedance Z_s have to be replaced with a parallel connection of impedance $2Z_s$. The entire filter structure can be converted using the identity shown in Figure 2, except the first and last impedance inverters and their adjacent shorted subs of impedance $2Z_s$.

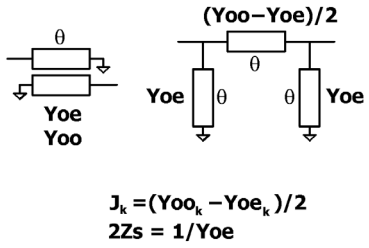

Figure 2. Circuit identity between a parallel-coupled shorted transmission-line section and a set of three uncoupled transmission-line sections. The equations below the schematic show how filter elements are related to the element values in the equivalent circuit. For simplicity, all impedances are normalized to Z_0 = 1 Ω; final values require denormalization.

To remove the last impedance inverter and shorted stub at each end of the filter structure, we propose the use of the third Kuroda identity shown in Figure 3 [18], for which the following holds:

$$\begin{aligned} 1/J'_k &= n/J_k \\ Z'_k &= nZ_k \\ n &= \frac{1}{1+\frac{1/J_k}{Z_k}} \end{aligned} \tag{5}$$

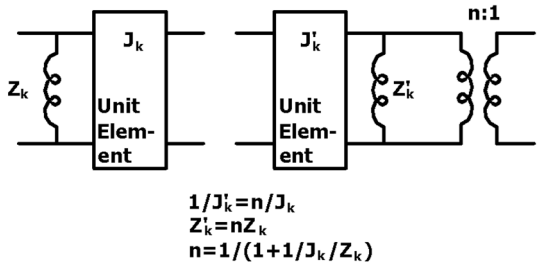

Figure 3. Third Kuroda identity allowing a shorted transmission-line stub to be moved across a unit element. The unit element's admittance equals the inverter value J_k from the filter schematic.

As shown, this identity allows the shorted stub to be shifted across the unit element, introducing an additional transformer. To maintain symmetry and obtain equal impedances

one must split the stub impedance $2Z_s$ into two values such that, after one is shifted across the inverter, both resulting stubs have equal impedance. The application of the third Kuroda identity is schematically shown in Figure 4. First, from the original circuit (Figure 4a), an additional transformer is extracted. Since it is connected directly to the resistive load, its effect is similar in nature to a unit element (which at the center frequency and for a resistive load, simply modifies the load value). To ensure the circuit response remains unchanged, the unit element's value is accordingly modified.

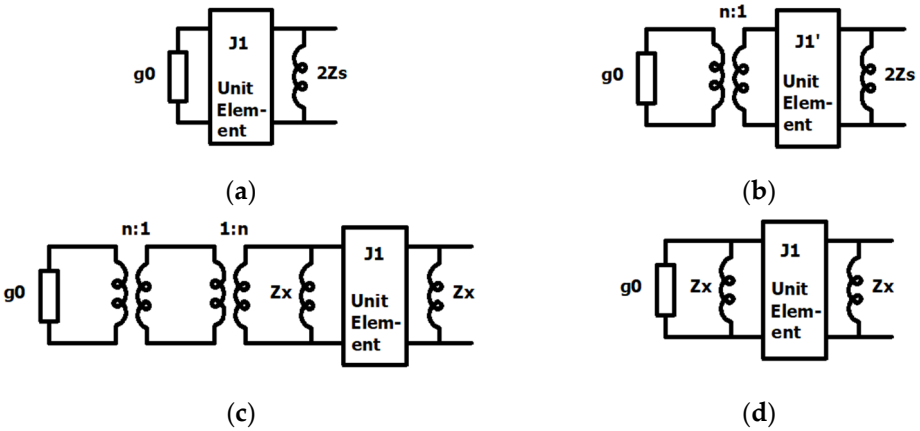

Figure 4. Transformation of the input/output of the bandpass filter to a structure suitable for parallel-coupled resonator filter design. Original filter input/output section (**a**); extraction of the input transformer (**b**); application of the third Kuroda identity (**c**); the final input/output filter network after transformers annihilation (**d**).

In the second step, the impedance stub $2Z_s$ is divided into two impedances, such that, when one of them is brought across the unit element, both stubs become equal in value. Also, the introduced transformer should be the inverse of the one introduced in the first step so they annihilate each other. The extracted transformer can be calculated as:

$$n = \frac{1}{2}\left(\frac{1/J_1}{2Z_s} + \sqrt{\Delta}\right) \tag{6}$$

where $\Delta = \left(\frac{1/J_1}{2Z_s}\right)^2 + 4$.

The impedance of the input/output stubs becomes:

$$Z_x = 2Z_s\left(\frac{1}{n} + 1\right) \tag{7}$$

Note: The inverter value J_1 does not change with this transformation scheme.

This completes the transformation of the filter, which is now ready for the application of the circuit identity from Figure 2, assuming ideal admittance inverters are replaced by appropriate circuit approximations. The final filter structure is shown in Figure 5. Some distortions may occur relative to the ideal filter from Figure 1c, due to replacing two ideal admittance inverters with unit elements. However, tuning Z_s (Z_x) can restore the desired filter response. The following condition provides the ideal response of the transformed filter:

$$J_1 = 1 - 1/Z_x \tag{8}$$

This condition has been derived by equating the magnitude of $ABCD_{22}$ parameters for the circuits in Figure 4a,d. The next subsections describe two possible admittance inverter approximations.

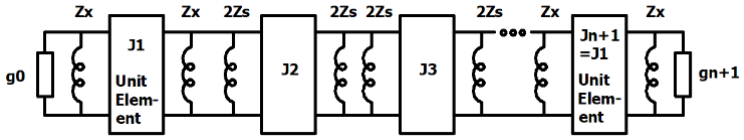

Figure 5. Schematic diagram of the complete transformed bandpass filter with ideal admittance inverters and two unit elements.

3.2. Narrowband Approach

In narrowband filter design, narrowband inverters can be used. All remaining inverters can then be replaced with the quarter-wavelength transmission-line sections with characteristic impedances equal to $1/J_x$. This method is suitable for filters with bandwidths up to 15%. A schematic diagram of such a realization is shown in Figure 6. In this case, condition (8) no longer holds due to distortions introduced by the unit elements. However, manual tuning of Z_s can yield an equal-ripple response.

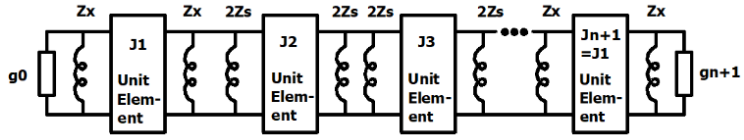

Figure 6. Schematic diagram of the narrowband bandpass filter with unit elements.

3.3. Broadband Approach

For broadband filter designs, broadband impedance inverters can be applied. Exemplary realizations of such inverters are described in [17]; they typically consist of a unit element with two shorted stubs that have negative characteristic impedance, as shown in Figure 7. With broadband inverters, bandwidths of up to 70% are achievable, with responses close to the ideal filter. As before, single-parameter tuning of Z_s (Z_x) leads to an equal ripple response. Condition (8) holds with negligible errors for bandwidths up to approximately 45%; above this value, manual tuning is required. Stub values are calculated as a parallel connection of the Z_s (Z_x) and inverter values J_k:

$$Z_k = 1/J_k || Z_k = \frac{-\frac{Z_k}{J_k}}{\frac{1}{J_k} - Z_k}, \; k = 1, \ldots, n+1 \tag{9}$$

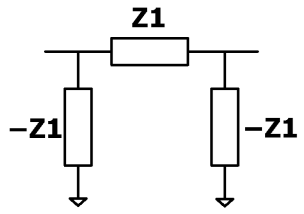

Figure 7. Broadband impedance inverter [17].

The filter structure is shown in Figure 8.

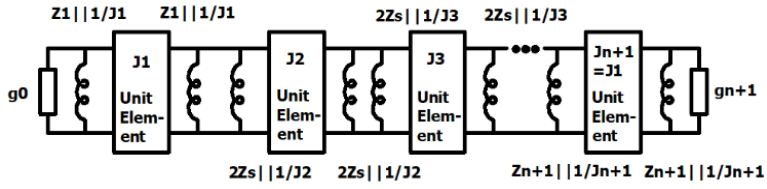

Figure 8. Schematic diagram of the broadband bandpass filter with unit elements.

4. Filter Performance Comparison and Discussion

To briefly present the effectiveness of the proposed method for parallel-coupled filter design, the frequency characteristics were calculated for two cases: (i) a narrowband filter with a bandwidth of 5% and (ii) a broadband filter with a bandwidth of 50%. The proposed method was compared with the most commonly used method published in [19], Section 8.09. The results of the calculations are presented in Figure 9. As can be observed, the proposed method allows for obtaining proper equal-ripple responses of the filter regardless of the filter's bandwidth, while the method from [19] produces proper responses only for narrowband filters. For moderate and wide bandwidths, the responses degrade significantly. There are known methods that are adequate for broadband filters, such as the one presented in [19], Section 10.02. However, such filters require quarter-wavelength filter sections of unequal strip widths. This is inconvenient because models of coupled sections with unequal width, though known in the literature, are not implemented in the majority of CAD software tools ver. 22.1 (17.04r build 17603 Rev 1) for microwave circuit design. Moreover, the calculation of the physical dimensions of asymmetric coupled sections is more troublesome than symmetric ones. In this respect, such methods are not very practical.

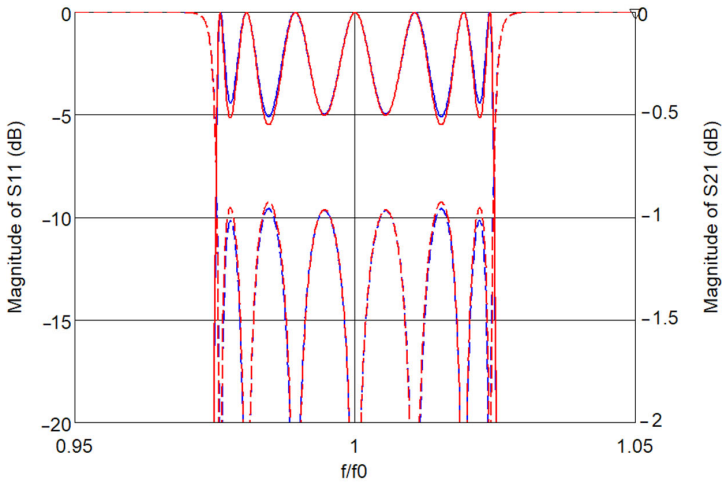

(**a**)

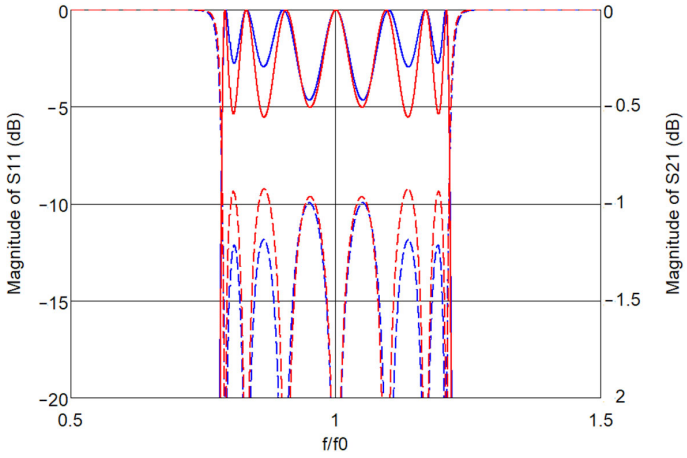

(**b**)

Figure 9. Calculated frequency characteristic of the 7th-order parallel-coupled filter using the proposed method (red lines) and the commonly known method described in [19], Section 8.09 (blue lines) for the narrowband case (B = 5%) (**a**); and the broadband case (B = 50%) (**b**). Solid lines—magnitude of S21; dashed lines—magnitude of S11.

To summarize, the proposed method is capable of producing accurate frequency responses regardless of the assumed bandwidth of the filter and can be realized with parallel-coupled symmetric sections (i.e., sections with equal strip widths).

5. Experimental Results

To experimentally verify the proposed design methodology, two parallel-coupled shorted resonator filters were designed, fabricated, and measured. The first example is a 5th-order filter with an in-band insertion loss ripple of 0.5 dB, a bandwidth of 10% and a center frequency of 2 GHz. This filter was designed using the narrowband approach and an arbitrary value of Z_s, without additional tuning. The electrical parameters of the filter are provided in Table 1, while Table 2 presents the calculated geometries of the coupled-line sections, based on their modal impedances. The geometry calculations were carried out using the TX Line transmission line calculator within the AWR Microwave Office software suite by Cadence Design Systems, Inc., San Jose, CA, USA, ver. 22.1 (17.04r build 17603 Rev 1). The theoretical frequency responses, modeled using ideal parallel coupled resonators described by their modal impedances Z_{oe} and Z_{oo}, are shown in Figure 10, alongside the corresponding measured responses.

Table 1. Electrical parameters of the 5th-order parallel-coupled filter: prototype conductance values g_k, normalized (Z_0 = 1 Ω) admittance inverter values J_k, stub impedances Z_k and modal impedances Z_{oe} and Z_{oo}.

k	g_k	J_k [S]	Z_k [Ω]	Z_{oe} [Ω] = $1/Y_{oe}$	Z_{oo} [Ω] = $1/Y_{oo}$
1	1.706	0.3172	1.29	1.29	0.7096
2	1.23	0.1185	1	1	0.8084
3	2.541	0.0971	1	1	0.8374
4	1.23	0.0971	1	1	0.8374
5	1.706	0.1185	1	1	0.8084
6	-	0.3172	1.29	1.29	0.7096

Table 2. Geometrical dimensions of the designed 5th-order parallel-coupled filter.

k	Coupled-Line Width [mm]	Coupled-Line Slot [mm]	Coupled Section Length [mm]
1	2.99	0.26	21.82
2	4.04	1.46	20.96
3	4.08	1.76	20.91
4	4.08	1.76	20.91
5	4.04	1.46	20.96
6	2.99	0.26	21.82

The second example is a 3rd-order filter with an in-band insertion loss ripple of 0.5 dB, a bandwidth of 30%, and a center frequency of 2 GHz. This filter was designed using the broadband approach, employing the broadband inverters shown in Figure 7, and applying the correction condition (8). The electrical parameters are listed in Table 3, and the geometrical parameters in Table 4. The theoretical and measured frequency responses are shown in Figure 11.

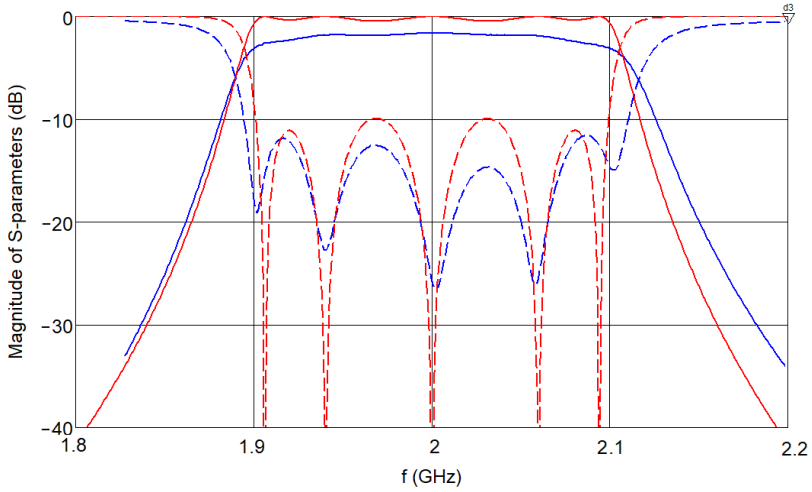

Figure 10. Calculated (red lines) and measured (blue lines) frequency responses of the 5th-order parallel-coupled filter using parameters listed in Table 1. Solid lines—magnitude of S21; dashed lines—magnitude of S11.

Table 3. Electrical parameters of the 3rd-order parallel-coupled filter.

k	g_k	J_k [S]	Z_k [Ω]	Z_{oe} [Ω] = 1/Y_{oe}	Z_{oo} [Ω] = 1/Y_{oo}
1	1.5963	2.079	1.925	1.925	0.675
2	1.0969	3.583	2.04	2.04	0.9539
3	1.5963	3.583	2.04	2.04	0.9539
4	-	2.079	1.925	1.925	0.675

Table 4. Geometrical dimensions of the designed 3rd-order parallel-coupled filter.

k	Coupled-Line Width [mm]	Coupled-Line Slot [mm]	Coupled Section Length [mm]
1	1.52	0.057	23.9
2	1.36	0.303	23.78
3	1.36	0.303	23.78
4	1.52	0.057	23.9

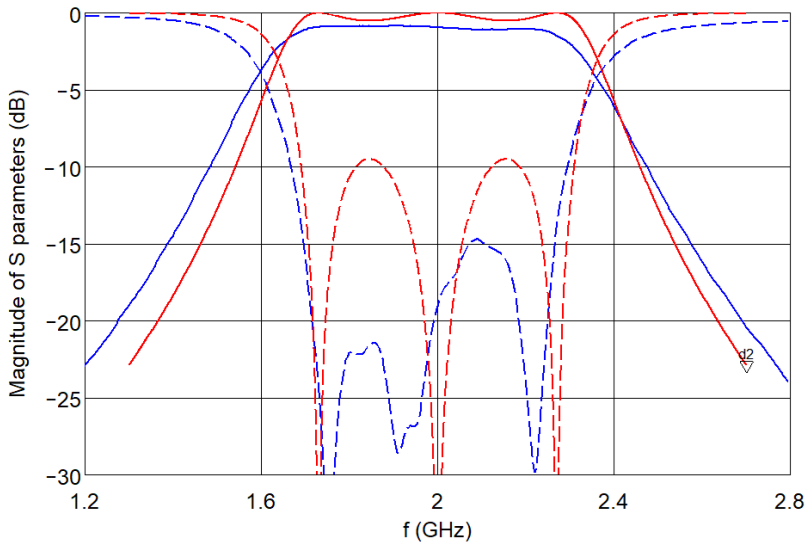

Figure 11. Calculated (red lines) and measured (blue lines) frequency responses of the 3rd-order parallel-coupled filter with the electrical parameters listed in Table 3. Solid lines—magnitude of S21; dashed lines—magnitude of S11.

Both filters were fabricated on Rogers RO4003C laminate (Rogers Corporation, Chandler, AZ, USA) with a thickness of 60 mils, and manufactured using the LPKF ProtoLaser S4 System (LPKF, Garbsen, Germany). Connections were implemented using laser-cur through-holes. Shorting pins (Bungard) were manually placed and fixed using a hand press.

The measured responses show good agreement with the theoretical predictions. The primary discrepancies arise from insertion loss caused by dielectric, conduction, and radiation losses. Notably, since the filters were measured without electromagnetic shielding, radiation is believed to be the main contributor to the passband losses, particularly because of the relatively large physical size of the structure compared to the guided wavelength.

In case of the 3rd-order filter, measured return losses outperform the theoretical ones. This is likely due to minor fabrication inaccuracies, particularly in tight gaps (as small as 0.057 mm) which approach the limit of manufacturing precision. These small gaps significantly influence return loss performance. Figure 12 shows the pictures of the fabricated filters with parallel-coupled shorted sections. To allow for filter measurements coaxial connectors were added to the input lines of the filter circuits. The transitions between microstrip and coaxial lines have not been de-embedded from the measurement, so some of the observed discrepancy between the measurements and theoretical responses may result from the introduced parasitics.

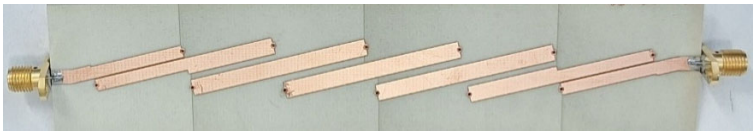

(**a**)

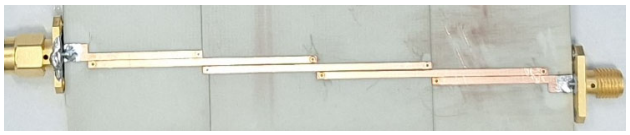

(**b**)

Figure 12. Photographs of the fabricated filters with shorted parallel-coupled sections. The 5th-order filter designed with the narrowband approach (**a**), and the 3rd-order filter designed with the broadband approach (**b**).

6. Conclusions

In this paper, a novel and practical approach for the design of microwave bandpass filters based on parallel-coupled shorted resonator has been presented. Unlike traditional methods, the proposed technique avoids the use of image parameter-based synthesis for filter element derivation. It has been demonstrated that the methodology outlined in [17] can be extended and improved by calculating admittance inverter values in a way that ensures all impedance stubs are equal. This introduces an additional degree of freedom in the design process, simplifying implementation and optimization.

A detailed transformation procedure has been developed to convert the general filter topology into one compatible with realization using parallel-coupled lines. By employing the third Kuroda identity, the original filter structure has been reconfigured into an equivalent network suitable for implementation using coupled-line equivalents. This transformation inherently involves the substitution of ideal admittance inverters with unit elements, which introduces distortion into frequency response, particularly for broadband filters. However, it has been shown that this effect can be mitigated by a simple single-parameter correction to the stub impedance, preserving the ideal response. A design condition based on the equivalence of ABCD matrix parameters has also been derived

to calculate the corrected stub impedance values, ensuring accurate filter responses for bandwidths up to approximately 45%. For wider bandwidths, additional tuning of the stub impedance allows for nearly ideal filter behavior.

The proposed method has been validated through the design, fabrication, and measurement of two prototype filters: a 5th-order narrowband filter employing quarter-wave inverters and a 3rd-order broadband filter incorporating broadband inverter structures. The measured responses of both designed filters closely match the theoretical predictions, with discrepancies attributed to expected physical effects such as conductor loss, dielectric loss, radiation, microstrip to coaxial line transitions, and fabrication tolerances.

Overall, the presented approach enables the reliable design of narrowband and broadband bandpass filters using symmetric parallel-coupled-line sections, while offering practical advantages in terms of implementation, CAD compatibility, and performance predictability.

Author Contributions: Conceptualization, methodology, formal analysis, investigation: S.G.; validation, experimental investigation: K.W.; writing—original draft preparation, S.G. and K.W. All authors have read and agreed to the published version of the manuscript.

Funding: This research was funded by The Ministry of Science and Higher Education, Republic of Poland, under research subsidy.

Data Availability Statement: Data are contained within the article.

Acknowledgments: The research results presented in this paper have been developed with the use of equipment financed from the funds of the "Excellence Initiative—Research University" program at AGH University of Krakow.

Conflicts of Interest: The authors declare no conflicts of interest.

References

1. Gomez-Garcia, R.; Yang, L.; Malki, M.; Munoz-Ferreras, J.-M. Frequency-Transformation-Based Co-Designed Lowpass-single/multi-passband highpass RF filters. *IEEE Trans. Circuits Syst. I Regul. Pap.* **2024**, *71*, 3608–3621. [CrossRef]
2. He, Y.; Cheng, L.; Xiao, L.; Ren, X.; Zhao, X.; Sun, L. Iterative synthesis of dual-band filters with separately assignable operating bands using bandpass polynomials and prototypes. *IEEE Microw. Wirel. Technol. Lett.* **2025**, *35*, 43–46. [CrossRef]
3. Bonizec, A.; Benedicto, J.; Favennec, J.-F.; Rius, E.; Goujon, C. Quarter-wavelength two-section coaxial stepped impedance resonators for harmonics suppression in Tx bandpass filters. *IEEE Access* **2025**, *13*, 9391–9398. [CrossRef]
4. Fang, Y.; Wu, J.; He, L.; Yang, H. A compact folded slotline bandpass filter based on SSPPs with improved out-of-band rejection. *IEEE Photonics Technol. Lett.* **2025**, *37*, 85–88. [CrossRef]
5. Tang, W.S.; Zheng, S.Y.; Pan, Y.M. Inline quasi-elliptic dielectric resonator filters with mixed coupling using dielectric junction. *IEEE Trans. Microw. Theory Tech.* **2024**, *72*, 6900–6913. [CrossRef]
6. Lee, S.; Lee, J.; Lee, B.; Lim, J.; Han, J.; Lee, J. K-band waveguide resonator bandpass filter structure with adjustable transmission zeros for producing various symmetric and asymmetric responses. *IEEE Access* **2025**, *13*, 8664–8675. [CrossRef]
7. Miljanovic, D.M.; Potrebic, M.M.; Tošic, D.V. Microwave bandpass filter with quasi-lumped elements. In Proceedings of the 23rd Telecommunications forum TELFOR 2015, Serbia, Belgrade, 24–26 November 2015; pp. 551–558. [CrossRef]
8. Liu, S.; Cheong, P.; Choi, W.-W. Synthesis of wideband bandpass filter with optimized matrix scaling for direct circuit implementation using lumped elements. *IEEE Microw. Wirel. Technol. Lett.* **2025**, *35*, 23–26. [CrossRef]
9. Wang, Y.; Fu, Y.; Liu, Q.; Dong, S.-W. Design of a substrate integrated waveguide bandpass filter using in microwave communication systems. In Proceedings of the ICMMT, Chengdu, China, 8–11 May 2010; pp. 1952–1954. [CrossRef]
10. Choi, H.; Song, M.; Lee, J. Novel transmission-line circuit configuration of cross-coupled filter with negative coupling. *IEEE Trans. Microw. Theory Tech.* **2024**, *72*, 4842–4853. [CrossRef]
11. Rao, J.; Sun, C.; Lu, J.; Gao, Q.; Zhou, B.; Zhao, H.; Liu, H.; Zhang, S.; Vaitukaitis, P.; Wang, L.; et al. Analysis of the metal plate coupled resonator with its compact in-line filter design applications. *IEEE Trans. Microw. Theory Tech.* **2024**, *72*, 5455–5466. [CrossRef]
12. Lu, Q.; Sun, J.; Zhang, H.; Zhang, T.; Zhu, Z. W-band compact triple-mode bandpass filter using multistub resonator in 65-nm CMOS technology. *IEEE Microw. Wirel. Technol. Lett.* **2024**, *34*, 1319–1322. [CrossRef]
13. Jamshdi-Zarmehri, H.; San-Blas, Á.A.; Neshati, M.H.; Cogollos, S.; Sharma, A.; Boria, V.E.; Coves, Á. Efficient design procedure for combline bandpass filters with advanced electrical responses. *IEEE Access* **2023**, *11*, 52168–52183. [CrossRef]

14. Cohn, S.B. Direct-coupled-resonator filters. *Proceeding IRE* **1957**, *45*, 187–196. [CrossRef]
15. Cohn, S.B. Parallel-coupled transmission-line-resonator filters. *IRE Trans. Microw. Theory Tech.* **1958**, *6*, 223–231. [CrossRef]
16. Matthaei, G.L. Design of wide-band (and narrow-band) band-pass microwave filters on the insertion loss basis. *Proceeding IRE* **1960**, *8*, 580–593. [CrossRef]
17. Gruszczynski, S.; Wincza, K. Broadband impedance inverters for application in synthesis and realization of bandpass filters. *IEEE Access* **2024**, *12*, 83260–83268. [CrossRef]
18. Ozaki, H.; Ishii, J. Synthesis of a class of strip-line filters. *IRE Trans. Circuit Theory* **1951**, *CT–5*, 104–109. [CrossRef]
19. Matthaei, G.L.; Young, L.; Jones, E.M.T. *Microwave Filters, Impedance Matching Networks and Coupling Structures*; McGraw-Hill: New York, NY, USA, 1964.

Disclaimer/Publisher's Note: The statements, opinions and data contained in all publications are solely those of the individual author(s) and contributor(s) and not of MDPI and/or the editor(s). MDPI and/or the editor(s) disclaim responsibility for any injury to people or property resulting from any ideas, methods, instructions or products referred to in the content.